PERSONALIZED ORODISPERSIBLE FILMS BY HOT MELT RAM EXTRUSION 3D PRINTING

Umberto M. Musazzi[1], Francesca Selmin[1], Marco A. Ortenzi[2], Garba Khalid Mohammed[1], Silvia Franzé[1], Paola Minghetti[1] and Francesco Cilurzo[1]*

[1] Department of Pharmaceutical Sciences, Università degli Studi di Milano - via G. Colombo 71 – 20133 Milan (Italy)
[2] Department of Chemistry, Università degli Studi di Milano - via Golgi, 19 – 20133 Milan (Italy)

*** to Whom the correspondence should be sent:**
Prof. Francesco Cilurzo, PhD
Department of Pharmaceutical Science
Università degli Studi di Milano
Via Giuseppe Colombo, 71
20133 Milano (I)
Phone: +39 02 503 24645
Fax: +39 02 503 24657
Email: francesco.cilurzo@unimi.it

Abstract:

This work demonstrated the feasibility of the extemporaneous preparation of maltodextrins orodispersible films (ODF) by hot-melt ram-extrusion 3D printing. This method consists of three simple technological operations which can be also implemented in a pharmacy setting. First, maltodextrins, drug, and other excipients are mixed in a mortar and wetted with the plasticizer (i.e. glycerine). Then, the mixture is fed in the chamber of the ram-extruder and heated. ODF are individually printed on the packaging material foil and sealed without further manipulations. The critical formulation attributes and process variables were investigated to define the processability space. In particular, the optimal conditions to print a mixture of maltodextrins/glycerine in 80/20 w/w ratio resulted: heating temperature: 85°C; needle gauge: 18 G; needle-packaging material foil distance: 0.6 mm; maximum print rate: 50 mm/s; filling angle: 120°. The maximum drug loading was about 40%, when paracetamol was used as model drug. The compounded ODF complied with USP and Ph. Eur. specifications for disintegration time (< 1 min). The dissolution pattern of paracetamol overlapped with that obtained from ODF with a similar composition prepared by the consolidated solvent casting technique, demonstrating the suitability of the proposed technology.

Keywords

Acetaminophen, compounding, edible film, immediate release, individualized therapy, orally disintegrating, tensile properties.

1 Introduction

Commercially available oral medicinal products do not satisfy all needs of special populations, such as dysphagics (Cilurzo et al., 2018), paediatrics (Visser et al., 2017), geriatrics (Scarpa et al., 2017) and patients with allergies or dietary restriction (Minghetti et al., 2015). In these cases, the drug has to be re-formulated or made from different inactive ingredients to comply the specific medical needs.

When the required dose is not available, the most common solution, which implies to split a solid dosage form, often occurs in dose inaccurancy (Casiraghi et al., 2014; Somogyi et al., 2017). The possible alternative is to compound a personalized drug product, e.g. solutions, syrups, capsules and tablets, in pharmacy settings. Despite this approach allows personalizing the dose, issues related to possible inaccuracy are only partially solved. As an example, the use of spoons or syringes would not allow the precise withdraw of the exact volume of liquids. On the other hands, the administration of tablets and capsules, which overcomes this drawback, can be associated with swallowing problems or fear of chocking and, in these cases, the patient compliance and the therapeutic adherence remain quite low (Cilurzo et al., 2018).

In the recent years, orodispersible dosage forms have been proposed in the personalization of the therapy (Visser et al., 2015), especially for children (Orlu et al., 2017) and elderly (Slavoka and Breitkreutz, 2015) due to the possibility of combining the advantages of solid dosage forms and liquid formulations. Despite both orodispersible tablets and films (ODF) can be currently compounded in pharmacy settings (Jha et al., 2011; Allen, 2016), the latter results are particular attractive since the dose is defined not only by the drug strength, but also by the dimensions of the ODF itself. In the selection of the appropriated manufacturing and/or compounding process, several technical and economic aspects have to be considered, e.g. the small batch production due limited number of dosage forms required for an individual patient, the cleaning procedure of the equipment to avoid the cross-contaminations, the number of critical process parameters to control during the

preparation and, last but not least, the necessity of a moisture proof packaging to protect ODF over the shelf-life.

In literature, both solvent casting and printing technologies have been proposed to prepare ODF. The former consist in a lab-coater apparatus that combines a doctor knife unit to assure the uniformity of thickness, and therefore of the drug content, to an oven to dry the slurry. Nevertheless, the residual moisture content in ODF is one of the main critical limitation of this strategy due to the impact on the film mechanical properties and stability (Musazzi et al., 2018). As an alternative, the simplest approach consists of depositing a known amount of a drug loaded polymeric slurry on a support, e.g. petri dish, flat moulds or unit-dose plate, drying in an oven and cutting the obtained film (Dinge and Nagarsenker, 2008, Liu et al., 2017; Foo et al., 2018;). In this case, the possible risks of dose inaccuracy are related to the lack of perfect alignment of the support base or the oven shelf that can cause the movement of the slurry and, therefore, a not-uniform film thickness. Ink-jet printing, which is based on the drug loading onto an edible film, is probably the widest explored printing technology to produce ODF. The feasibility of this approach was demonstrated with several drugs (Scarpa et al., 2017) also in fixed combinations (Thabet et al., 2018). Moreover, inkjet printing can enable the simultaneous and independent dosing of drug combinations, as demonstrated using triiodothyronine and thyroxine, easily recognized by adding two different colouring agents (Alomari et al. 2018). The addition of a colouring agent to the ink can also permit the simple visualization of the uniformity of printed structures and, therefore, drug content (Vakili et al., 2016). Despite these advantages, this technology cannot be easily applied to load poorly soluble drugs, since inks need to be formulated case-by-case to avoid the drug sedimentation, which is the main source of dose inaccuracy. Hence some Scarpa and co-workers opts to formulate not-aqueous solutions, nanosuspensions or lipidic inks (Scarpa et al., 2017). Alternatively, the melt ink-jet printing allows a good control of the drug solid state and film morphology (Içten et al., 2015; Içten et al., 2016) and the flexographic printing was also tested to impregnate placebo ODF with a precise dose of a drug (Janßen et al., 2013).

More recently, fused deposition modelling (FDM) 3D printing, which is usually explored to design solid oral dosage forms (Awad et al., 2018) with different geometries (Sadia et al., 2018) and release characteristics (Kadry et al., 2018) was also studied in the attempt to avoids the need of preformed films (Ehtezazi et al., 2018). Nevertheless, the application of such technology to the extemporaneous preparation of ODF could be very complicated because drug-loaded filaments have to be preliminarily produced by hot-melt extrusion (Cunha-Filho et al., 2017) or obtained by impregnation of commercial filament (Kadry et al., 2018) with all the limitation described by Fuenmayor and co-workers (2018).

This work describes a novel approach to print ODF intended for personalized therapy. The basic idea of the proposed technology arose from the combination of a hot melt ram extruder, able to extrude a drug/polymer/plasticizer blend, and the typical aligned plate of 3D printers whose movements allow the deposition material of the desired dimensions and shape. Maltodextrins were tested as the main component of the formulation since the possibility to obtain ODF by hot-melt extrusion is documented (Cilurzo et al., 2008) as well as the feasibility to tune the ODF mechanical properties by varying the maltodextrins molecular weight and/or the plasticizer ratio (Cilurzo et al., 2010; Cilurzo et al., 2011).

2 Materials and methods

2.1 Materials

Maltodextrins with a dextrose equivalent (D.E.) equal to 6 (Glucidex® IT6, MDX6) and 12 (Glucidex® IT12, MDX12) were kindly obtained by Roquette (France). Paracetamol (PAR), glycerine and titanium dioxide (TiO_2) were purchased from Farmalabor (Italy). Span® 80 was supplied from Croda (Spain). Glycine (GLY) was purchased from ACEF. (Italy). All solvents were of analytical grade unless specified.

2.2 Rheological characterization of maltodextrin/plasticizer blends

Compression tests – Tests were performed on 0.4 mm thick laminates made of MDX6 and glycerine in the 80/20 and 84/16 ratios in order to assess their softening temperature. Laminates were prepared by solvent casting technique by using a laboratory-coating unit Mathis LTE-S(M) (Swissland). MDX6 (75% w/w) and glycerine in water at 80 °C under stirring. After a rest period of at least 24 h to remove air bubbles, the aqueous dispersion was cast onto a silicone release liner with a 650 μm thickness. The coating rate was fixed at 1 m/min, and the cast dispersion was dried in the oven at 80 °C for 30 min with a horizontal air circulation speed of 1200 rpm.

Laminates were placed in the rheometer (Physica MCR 300 rheometer, Anton Paar GmbH, Austria) at 50 °C, compressed with a normal force of 10 N using a 25 mm upper plate and heated at the heating rate of 5 °C/min. The softening temperature was expressed as the onset of the curve resulting from the analysis.

Frequency sweep experiments - Tests were performed on selected ODF, among those reported in **Table 1**, from 100 to 0.1 Hz (angular frequency – ω of 620-0.628 s^{-1}) in the strain-controlled mode using a plate-plate geometry, 25 mm diameter at the temperature of 80, 90, 100 and 110 °C (Physica MCR 300 rheometer, Anton Paar GmbH, Austria). The strain was set at 5% to be in the linear viscoelastic regime of the blends. In order to estimate a possible relationship between the rheological data and the feasibility to print the designed formulations, the shear viscosity at 1.1 s^{-1}shear rate was calculated according to Cox-Merz rule. The shear rate value was also determined since it corresponds to the extrusion rate during the 3D printing of the ODF.

2.3 Preparation of ODF

Design of the printer - The printer was designed modifying a Cartesian FDM 3D printer (Futura Group Srl, Italy), as depicted in **Figure 1**. In particular, the apparatus used for the filament extrusion was replaced by in-house vertical ram extruder. The 60 mL extrudating chamber was thermostated in the range from 30 to 200 °C and ended with a Luer-lock system fitting 1.8 cm

length needles with a gauge ranging from 18 to 20 G. The melted materials extruded through the die was deposited on a 20×20 cm aluminium packaging foil. This foil also consisted in the primary packaging of ODF. The ram speed and the chamber temperature were controlled by Repetier-Host 2.0.1 software (Hotword GMBH, Germany); the film dimension and number per each print were designed by 3D builder (Microsoft, USA) and converted in G-code. Finally, ODF were sealed with another packaging foil without further manipulations.

Preparation of the mixture for printed ODF - The mixtures were obtained by mixing the exactly weighted amount of each component in a mortar according to the composition reported in **Table 1**. The final weight of each mixture was about 10 g.

Preparation of cast ODF - ODF containing 25% w/w paracetamol was also prepared by solvent casting technique and used as reference for dissolution studies. Briefly, an aqueous dispersion was prepared by mixing MDX6, glycerine, Span® 80 in distilled water at 80 °C under stirring. After at least 24 h of rest to remove air bubbles, the aqueous dispersion was cast onto a silicone release liner with a 150 μm thickness. The coating rate was fixed at 1 m/min, and the cast dispersion was dried in the oven at 80 °C for 30 min with a horizontal air circulation speed of 1200 rpm. The obtained cast ODF (formulation C1) had the following composition: 57 % w/w MDX6, 16 % w/w glycerine, 2 % w/w Span® 80, and 25% w/w paracetamol.

2.4 Physical characterization

Film thickness – The film thickness was measured by using a micrometer MI 1000 μm (ChemInstruments, USA).

Film stickiness – The ODF stickiness at different plasticizer contents was evaluated by the thumb tack test. Briefly, the thumb was pressed lightly on a film sample for a short time and, then, quickly withdrawn. By varying the pressure and time of contact and noting the difficulty of pulling the thumb from the adhesive, it is possible to perceive how easily, quickly and strongly the adhesive can form a bond with the thumb. All the tests were simultaneously performed and blind. The

stickiness of the ODF was expressed by the following score system: A (no sticky), B (sticky), and C (very sticky) (Musazzi et al., 2018).

Tensile properties – Tests were conducted according to ASTM International Test Method for Thin Plastic Sheeting (D 882-02) using an Instron 5965 texture analyzer (Instron, UK), equipped with a 50 N load cell. The film was cut into 80×15 mm strips and equilibrated at 25±1 °C for 1 week. Each test strip was longitudinal by placed in the tensile grips on the texture analyzer. Initial grip separation and the crosshead speed were 20 mm and 12.5 mm/min, respectively. The test was considered concluded at the film break. The following parameters were determined:

Tensile strength (TS) was calculated by dividing the maximum load by the original cross-sectional area of the specimen.

Percent elongation at break (E%) was calculated according to the following equation:

$$E\% = \frac{L - L_0}{L_0} \times 100$$

where L_0 is the initial gage length of the specimen and L is the length at the rupture.

Elastic modulus or Young's modulus (Y) was calculated as the slope of the linear portion of the stress-strain curve.

Tensile energy to break (TBE) was defined by the area under the stress-strain curve. The results were expressed in MPa.

2.5 Loss of drying

The loss on drying (LOD) in films was determined gravimetrically by using a thermobalance (Gilbertini, Italy). Film samples were kept at 105 °C until constant weight.

2.6 Disintegration test

The disintegration test was carried out in water according to specifications of the monograph on "Disintegration of tablets and capsules" reported in the Ph. Eur. The results complied the Ph. Eur. requirement for orodispersible tablets if the disintegration time was lower than 3 min.

2.7 Drug content

A 3×2 cm loaded ODF was dissolved in 100 mL purified water, sonicated for 10 min and diluted 1:10. Paracetamol content was determined spectrophotometrically at 243 nm (UV-Vis spectrometer, Lambda 25, Perkin Elmer, Italy). The calibration curves ranged from 10 to 100 µg/mL ($R^2 < 0.999$).

2.8 In vitro dissolution test

The in vitro dissolution test was carried out in a Ph. Eur. basket dissolution apparatus using 3×2 cm samples of paracetamol loaded ODF. The dissolution medium was 900 mL freshly deionized water, maintained at 37±1 °C and stirred at 50 rpm. Paracetamol concentrations were assayed spectrophotometrically at 243 nm (UV-Vis spectrometer, Lambda 25, Perkin Elmer, Italy) every 2 min and the calibration curve was in the range of 10-100 µg/mL ($R^2 < 0.999$). A loaded ODF prepared by solvent casting technique (25% w/w) was used as control. The results were expressed as the mean and standard deviation values of four replicas for each tested formulation.

3 Results and Discussion

3.1 Rheological characterizations

In order to determine the temperature range suitable for frequency sweep experiments, preliminary compression tests were performed on laminates made of MDX6. This material was supposed to present the highest softening temperature, having the highest M_w. The softening temperatures of laminates containing 20% w/w or 16% w/w glycerine were at about 79.5 °C and 99.7 °C,

respectively. Therefore, the temperature range of frequency sweep experiments was set in the range 80-110 °C. The results evidenced that all tested samples did not present a pseudo-plastic behaviour, i.e. no plateau viscosity was reached at low angular frequency, probably due to the high number of interactions arising among –OH groups. As an example, the rheological pattern of formulation 1 (MDX6/glycerine ratio: 80/20) is exemplified in **Figure 2.**

To estimate the possible behaviour of formulations upon printing, the shear viscosity was also measured The amount of the plasticizer was more relevant than the MDX molecular weight in determining the viscosity of the blend (**Table 2**). Furthermore, in agreement with the previous DSC data (Selmin et al., 2015), glycine significantly ameliorated the fluidity of the melted blends **(Table 2**).

3.2 Set-up of printing operative conditions

On the bases of the frequency sweep data the temperature for the hot-melt ram extrusion of formulations containing the 20% and 16% w/w glycerine was set at 85 °C and 95 °C, respectively. Moreover, based on the results of compression tests, a time lapse of 10 min between the mixture loading and the beginning of the ram movement was established to permit the complete melting of the formulation. The set-up of the operative conditions, the needle inner diameter, the relative distance between the extruder needle and the mobile plate, the speed of the mobile plate and the filling angle, was defined by using Formulation 4 and Formulation 9 (**Table 1**). In particular. Formulation 9, having the highest glycerine content, was selected to check the impact of fluidity of the melt on printability. Conversely, Formulation 4 was tested as a worst case since it contained the lowest amount of glycerine, glycine as non-traditional plasticizer and TiO_2 a very fine inert powder usually used to mask possible visual defects of ODF.

First, the extrusion of formulation 4 at the extrusion 1.1 s^{-1} shear rate was possible only using the 18 gauge-needle (inner diameter 0.838 mm). Secondly, the suitable deposition of the melted blend on packaging foil was possible only setting the distance from the needle tip to the surface of the

packaging material foilin the range of 0.5-0.8 mm. Indeed, at distances lower than 0.5 mm, the needle tip scratched the film causing irregularity and roughness on the surface, whilst at distances higher than 0.8 mm, the extruded material could not deposit in a consistent and uniform way. Thirdly, the impact of print rate on the film formation was investigated in the 10-50 mm/s range increasing the extrusion shear rate, accordingly. The maximum rate which allowed the deposition of a filament with a uniform diameter, resulted 12 mm/s and 50 mm/s for formulations 4 and 9, respectively.

Finally, the effect of the filling angle on the homogeneity and tensile properties of films was studied by printing at 90°, 120° 135°, 150° and 180° with respect to the X-axis of the packaging material foil (**Figure 3**). The results indicated that the filling angle did not affect the film appearance. In the case of formulation 4, some small differences were noticed in the main descriptors of the tensile property (**Table 3**), suggesting an influence of the filling angle on the film inner organization. Indeed, due to the peculiar preparation process, it was possible to speculate that the printed films had some high-dense zones at the deposition lines of extruded materials and some low-dense zones between the previous ones due to the reorganization of the melted materials after deposition. Therefore, toughness (e.g., TS and TBE) reached the highest values when the highly dense zones of the films were parallel to the tensile force applied (i.e., 180°). On the contrary, the lowest TBE values were determined when the dense material zones were perpendicular (i.e., 90°) since the film resistance to deformation was mainly limited by thin and low-dense zones, which were expected to be mechanically weak. Interestingly, ODF printed at the filling angle of 120° showed the highest field of elasticity (i.e., the lowest *Y* values) and a satisfactory toughness probably due to a cooperation between high-dense and low-dense zones during the elongation phase. A similar trend was observed in the case of formulation 9 printed at 120° confirming that the orientation of the high-dense and low-dense zones influenced the tensile properties (**Table 3**).

The comparison of the tensile data on these two formulations evidenced an anomalous result considering the plasticizer content. Indeed, the higher glycerine concentration, the lower the

ductility (E% values) and the tenacity of the film (TS). This feature can be attributed to glycine and TiO_2, which actas non-traditional plasticizers (Selmin et al., 2015) and nanofiller of maltodextrins (Franceschini et al., 2016), respectively.

On the bases of the obtained data, the following process parameters were set and used for further studies:

- needle gauge: 18;
- needle-to-packaging material foil distance: 0.6 mm;
- print rate: 12 mm/s;
- ram rate: 10 mm/s (corresponding to a calculated shear rate of the melted mixture of 1.1 s^{-1});
- filling angle: 120°.

3.3 ODF characterization

All printed films presented relatively low LOD values (**Table 1**) if compared to other formulations (Musazzi, 2018) and the thickness in the 150-250 μm range was considered suitable for patient's handling. Moreover, ODF dissolved within 3 min complying with Ph. Eur. specifications for orodispersible dosage forms (Ph. Eur., 2018a).

Although the tensile properties and stickiness of printed ODF are not as critical as for those industrially produced by solvent casting technique, which are rolled up on reels and cut, their investigation is worthy of interest to avoid problems during the patient's handling.

The data obtained during the definition of the process parameters evidenced an impact of mixture composition on the printability. The formulations containing 16% w/w glycerine were not consistently extruded through a 18 gauge-needle unless glycine was also added at the concentration of 2.5% or 1.25% w/w glycine for MDX6 (formulations 3 and 4) and MDX12 (formulation 6), respectively. These results suggested that the shear viscosity, calculated at 1.1 s^{-1} of shear rate, might be lower than 7 kPa*s. Nevertheless, formulations made of MDX12 (formulations 6 and 7) were stickier than those based on MDX6 (formulations 3 and 4) (**Table 1**), confirming the relevance

of the maltodextrin molecular weight. Moreover, in ODF prepared with MDX6 and the highest glycerine concentration, the concomitant presence of glycine increased the elasticity in a concentration-dependent way and had a negative impact on toughness. Indeed TS, TBE and *Y* values (**Table 4**) decreased in the following order: formulation 9 > formulation 11 > formulation 12 ($p < 0.05$).

As expected, the addition of TiO_2 (see formulation 3 vs. formulation 4; formulation 10 vs. formulation 9, **Table 4**) decreased the *Y* values suggesting that the peeling of film from the packaging foil should be easier.

Based on these results, some generic considerations on preparation methods and the ODF characteristics can be drawn. First, the disintegration time of printed ODF is more similar to that of films with similar composition, but prepared by hot-melt extrusion (≥ 45 s), rather than by solvent casting (≈ 10 s) (Cilurzo et al., 2008). Furthermore, the disintegration times (**Table 1**) were closed to the results reported for film prepared by FDM 3D printing (Ehtezazi et al., 2018; Jamroz et al., 2017). Secondly, the printed ODF showed weaker tensile properties than the parent casted and hot-melt extruded ODF probably because the peculiar deposition of melted material do not allow obtaining a uniform film in comparison to extrusion. As a consequence, the TS values of extruded ODF composed by MDX12, glycerine and cellulose microcrystalline in the 66:22:11 ratio (Cilurzo et al., 2008) resulted 5-fold higher than formulation 9. Moreover, the solvent casting technique allowed to obtain higher cohesion of the ODF matrix, since the maltodextrin chains and glycerine could rearrange in a dense structure during the solvent evaporation phase, resulting in a film with suitable mechanical properties even at thinner thickness.

It is noteworthy that the proposed maltodextrin ODF showed a higher elasticity and a lower toughness than that of PVA-based ones (Jamroz et al., 2017), while the overall tensile properties were similar to those of films made of PEO and starch (Ehtezazi et al., 2018).

When paracetamol was loaded as model drug, ODF appeared whitish without significant differences in thickness and weight (**Table 5**) or in the disintegration time with respect to the

corresponding placebo formulations (**Table 1**). Paracetamol could be loaded in ODF up to 35% w/w (**Table 5**) and in all cases the uniformity of dosage units was within the limit (L_1 ± 15%) set by the European Pharmacopoeia (Ph. Eur., 2018b).

In agreement with the literature data (Musazzi et al., 2018), the paracetamol loaded into ODF altered the tensile properties (**Table 4**) increasing the ODF toughness (e.g., TS; $p < 0.01$) and, consequently, decreasing its ductility (i.e., E%; $p < 0.02$) with respect to placebo formulations (i.e., formulations 4 and 9). However, this effect was not related to the paracetamol content since no significant differences in terms of TS, Y and E% values (formulations 13-15) were observed. However, a slight decrease of TBE values observed in 35% w/w drug loaded ODF ($p < 0.01$) suggested that a high payload can create inhomogeneous spot in the inner structure of an ODF causing the alterations of its mechanical properties (Musazzi et al., 2018).

As shown in the dissolution profiles reported in **Figure 4**, about 80% of paracetamol was dissolved within 6 min so that the proposed printed ODF can be classified as very rapidly dissolving dosage forms according to the FDA (FDA, 2017). However, slight differences were observed depending of plasticizer content since ODF containing 20% w/w glycerine dissolved faster ($t_{80\%} \leq 2$ min) than those with 16% ($t_{80\%} \approx 6$ min). The dissolution profiles resulted superimposable in comparison to Formulation C1 produced by casting technique. These results confirmed the ability of maltodextrins to improve the dissolution rate of several active ingredients such as piroxicam (Cilurzo et al., 2008), diclofenac (Cilurzo et al., 2011) and in some cases to enhance the mucosae permeation also in comparison with other film forming materials used to prepare ODF as demonstrated in the case of sumatriptan (Soni et al., 2015).

4 Conclusions

The feasibility to prepare MDX-ODF by hot melt ram extrusion 3D printing was demonstrated. The proposed preparation method consists of a simple procedure involving the mixing of the active ingredient with MDX and other excipients, the wetting of the mixed powders by glycerine, the

loading into the ram extruder and the printing of the single dosage form directly on the packaging foil. This aspect is relevant since the printed ODF can be sealed with another packaging foil avoiding handling of the dosage form. The drug strength can be easily defined designing the size of ODF. The uniformity of drug amount per unit of these medicinal products should be guarantee aiming to serve the interest of patients. Conversely to the industrial products, the drug strenght cannot be quantified due to the limitation of pharmacy equipment, time and costs (Resolution CM/Res(2016)1). As proposed for ink-jet printing, the drug homogeneity in the wet mixture could be indirectly checked by adding small amounts of colourant during the mixing, which is the most critical operation. Indeed, variation in ODF thickness and dimensions, can be indirectly determined gravimetrically.

The proposed method also appears to be more versatile than FDM 3Dprinting, where it is necessary to produce drug loaded filaments, to obtain the final object. With respect to the ink-jet printing technologies, the proposed approach presents the advantage to not require the preliminary preparation of placebo ODF. Moreover, avoiding the use of solvents, this method also reduces the risks of drug polymorphism. Based on this evaluation, we consider this method as a good opportunity to extemporaneously prepare tailored solid dosage forms in hospital and community pharmacies.

Figure captions

Figure 1 – The main features of hot melt ram extrusion 3D printer.

Figure 2 – Frequency sweeps curves of formulation 9 performed at 80 °C, 90 °C, and 110 °C.

Figure 3 – Schemes of filling angles of 3D printed films.

Figure 4 – Dissolution profiles of paracetamol from ODF obtained by 3D printing (formulations F8, F13-15) and casting solvent technology (formulation C1) (mean ± St.Dev., n = 4).

Bibliography

Allen L.V., 2016. Basics of compounding: compounding films. Int. J. Pharm. Compd. 20 (4), 298-305.

Alomari M., Vuddanda P. R., Trenfield S. J., Dodoo C. C., Velaga S., Basit A. W., Gaisford S., 2018. Printing T_3 and T_4 oral drug combinations as a novel strategy for hypothyroidism, Int. J. Pharm., 549(1-2), 363-369.

Awad, A., Trenfield, S.J., Goyanes, A., Gaisford, S., Basit, A.W., 2018. Reshaping drug development using 3D printing. Drug Discov. Today. 23, 1547-1555.

Casiraghi A., Musazzi U.M., Franceschini I., Berti I., Paragò V., Cardosi L., Minghetti, P., 2014. Is propranolol compounding from tablet safe for pediatric use? Results from an experimental test. Minerva Pediatrica 66(5), 355-362.

Cilurzo F., Cupone I.E., Minghetti P., Selmin F., Montanari L., 2008. Fast dissolving films made of maltodextrins. Eur. J. Pharm. Biopharm. 70 (3), 895-900.

Cilurzo F., Cupone I.E., Minghetti P., Buratti S., Selmin F., Gennari C.G.M., Montanari L., 2010. Nicotine fast dissolving film made of maltodextrins: a feasibility study. AAPS PharmSciTech 11(4), 1511-1517.

Cilurzo F., Cupone I.E., Minghetti P., Buratti S., Gennari C.G.M., Montanari L., 2011. Diclofenac fast-dissolving film: suppression of bitterness by a taste-sensing system. Drug Dev. Ind. Pharm. 37(3), 252-259.

Cilurzo F., Musazzi U.M., Franzé S., Selmin F., Minghetti P., 2018. Orodispersible dosage forms: biopharmaceutical improvements and regulatory requirements. Drug Discov. Today 23(2), 251-259.

Cunha-Filho M., Araújo M.R., Gelfuso G.M., Gratieri T., 2017. FDM 3D printing of modified drug-delivery systems using hot melt extrusion: a new approach for individualized therapy. Ther. Deliv. 8(11), 957-966.

Davidek T., Marabi A., Mauroux O., Bauwens I., Kraehenbuehl K., 2018. Preparation of activated flavor precursor DFG, N-(1-deoxy-1-fructosylglycine) by combination of vacuum evaporation and closed system heating steps. Food Chemistry 244, 177-183.

Dinge A., Nagarsenker M., 2008. Formulation and evaluation of fast dissolving films for delivery of triclosan to the oral cavity. AAPS PharmSciTech 9(2), 349-356.

Ehtezazi T., Algellay M., Islam Y., Roberts M., Dempster N.M., Sarker S.D., 2018. The application of 3D printing in the formulation of multi-layered fast dissolving films. J. Pharm. Sci. 107, 1076 1085.

European Pharmacopeia (Ph. Eur.), 2018a. Monograph on Tablets (01/2018:0478). In European Pharmacopeia, 9th Edition Supplement 9.5.

European Pharmacopeia (Ph. Eur.), 2018b. Monograph on Uniformity of Dosage Units (04/2017:20940). In European Pharmacopeia, 9th Edition Supplement 9.5.

Food and Drug Administration (FDA), 2017. Waiver of in vivo bioavailability and bioequivalence studies for immediate-release solid oral dosage forms based on a biopharmaceutics classification system (Guidance for industry).

Foo W.C., Khong Y.M., Gokhale R., Chan S.Y., 2018. A novel unit-dose approach for the pharmaceutical compounding of an orodispersible film. Int. J. Pharm. 539, 165-174.

Fuenmayor E., Forde M., Healy V.A., Devine M.D., Lyons G.J., McConville C., Major I., 2018. Material considerations for fused-filament fabrication of solid dosage forms. Pharmaceutics. 10(2), 44

Franceschini I., Selmin F., Pagani S., Minghetti P., Cilurzo F., 2016. Nanofiller for the mechanical reinforcement of maltodextrins orodispersible films. Carbohydrate Polymers 136, 676-681.

Goyanes A., Scarpa M., Kamlow M., Gaisford S., Basit A.W., Orlu M., 2017. Patient acceptability of 3D medicines. Int. J. Pharm. 530, 71-78.

Kadry H., Al-Hilal T.A, Keshavarz A., Alam F., Xu C., Joy A., Ahsan F., 2018. Multi-purposable filaments of HPMC for 3D printing of medications with tailored drug release and timed-absorption, Int J Pharm. 544(1), 285-296.Içten E., Giridhar A., Taylor L.S., Nagy Z.K., Reklaitis G.V., 2015. Dropwise additive manufacturing of pharmaceutical products for melt-based dosage forms. J. Pharm. Sci. 104(5), 1641–1649.

Içten E., Giridhar A., Nagy Z.K., Reklaitis G.V., 2016. Drop-on-demand system for manufacturing of melt-based solid oral dosage: effect of critical process parameters on product quality. AAPS PharmSciTech 17(2), 284-293.

Jamroz W., Kurek M., Lyszczarz E., Szafrenic J., Knapik-Kowalczuk J., Syrek K., Paluch M., Jachowich R., 2017. 3D printed orodispersible films with Aripiprazole. Int. J. Pharm. 533, 413-420.

Janßen E.M., Schliephacke R., Breitenbach A., Breitkreutz J., 2013. Drug-printing by flexographic printing technology—A new manufacturing process for orodispersible films. Int. J. Pharm. 441(1–2), 818-825.

Jha A.K., Chetia D., 2011. Development and statistical analysis of glipizide loaded fast-dissolving tablets using Plantago ovata husk as a superdisintegrant. Int. J. Pharm. Compd. 15(6), 521-525.

Liu C., Chang D., Zhang X., Sui H., Kong Y., Zhu R., Wang W., 2017. Oral fast-dissolving films containing lutein nanocrystals for improved bioavailability: formulation development, in vitro and in vivo evaluation. AAPS PharmSciTech 18, 2957-2964.

Minghetti P., Pantano D., Gennari C.G.M., Casiraghi A., 2014. Regulatory framework of pharmaceutical compounding and actual developments of legislation in Europe. Health Policy 117(3), 328-333.

Musazzi U.M. Selmin F., Franzé S., Gennari C.G.M., Rocco P., Minghetti P., Cilurzo F., 2018. Poly(methyl methacrylate) salt as film forming material to design orodispersible films. Eur. J. Pharm. Sci. 115, 37-42.

Orlu M., Ranmal S.R., Sheng Y., Tuleu C., Seddon P., 2017. Acceptability of orodispersible films for delivery of medicines to infants and preschool children. Drug Delivery 24(1), 1243-1248.

Preis M., Woertz C., Kleinebudde P., Breitkreutz J., 2014. Oromucosal film preparations: classification and characterization methods. Expert Opin. Drug Deliv. 10(9), 1303-1317.

Resolution CM/Res(2016)1 on quality and safety assurance requirements for medicinal products prepared in pharmacies for the special needs of patients.

Sadia M., Arafat B., Ahmed W., Forbes R.T., Alhnan M.A, 2018. Channelled tablets: An innovative approach to accelerating drug release from 3D printed tablets. J. Control. Rel. 269, 355-363.

Scarpa M., Stegemann S., Hsiao W.-K., Pichler H., Gaisford S., Bresciani M., Paudel A., Orlu M., 2017. Orodispersible films: towards drug delivery in special populations. Int. J. Pharm. 523(1), 327-335.

Selmin F., Franceschini I, Cupone IE, Minghetti P, Cilurzo F., 2015. Aminoacids as non-traditional plasticizers of maltodextrins fast-dissolving films. Carbohyd. Pol. 115, 613-616.

Slavkova M., Breitkreutz J., 2015. Orodispersible drug formulations for children and elderly. Eur. J. Pharm. Sci. 75, 2-9.

Somogyi O., Meskó A., Csorba L., Szabó P., Zelkó R., 2017. Pharmaceutical counselling about different types of tablet-splitting methods based on the results of weighing tests and mechanical development of splitting devices. Eur. J. Pharm. Sci. 106, 262-273.

Soni, G., Yadav, K.S., 2015. Fast-dissolving films of sumatriptan succinate: factorial design to optimize in vitro dispersion time. J. Pharm. Innov. 10, 166-174.

Thabet Y., Lunter D., Breitkreutz J., 2018. Continuous inkjet printing of enalapril maleate onto orodispersible film formulations. Int. J. Pharm. 546, 180–187.,

Goyanes A., Vakili H., Nyman J.O., Genina N., Preis M., Sandler N., 2016. Application of a colorimetric technique in quality control for printed pediatric orodispersible drug delivery systems containing propranolol hydrochloride. Int. J. Pharm. 511, 606–618.

Visser J.C., Woerdenbag H.J., Crediet, S., Gerrits, E., Lesschen, M.A., Hinrichs, W.L.J., Breitkreutz, J., Frijink H.W., 2015. Orodispersible films in individualized pharmacotherapy: the development of a formulation for pharmacy preparations. Int. J. Pharm. 478, 155-163.

Visser J.C., Woerdenbag H.J., Hanff L.M., Frijlink H.W., 2017. Personalized medicine in pediatrics: the clinical potential of orodispersible films. AAPS PharmSciTech 18, 267-272.

Wening K., Breitkreutz J., 2011. Oral drug delivery in personalized medicine: unmet needs and novel approaches. Int. J. Pharm. 404, 1-9.

Table 1 – Composition of placebo and paracetamol (PAR) loaded ODF obtained by 3D printing. The main components were maltodextrins with a dextrose equivalent of 6 (MDX6) and 12 (MDX12), glycerine (GLN), glycine (GLY) and titanium dioxide (TiO_2). Loss of drying (LOD) and disintegration time (Disgr) are enlisted. The ODF stickiness is expressed by the following score system: A (no sticky), B (sticky), and C (very sticky).

Form	ODF composition (%, w/w)						LOD	Stickiness	Disgr.
	MDX6	MDX12	GLN	GLY	PAR	TiO_2	(%, w/w)	(A, B, C)	(s)
1	84.00	-	16.00	-	-	-	-*	-*	-*
2	82.75	-	16.00	1.25	-	-	-*	-*	-*
3	81.50	-	16.00	2.50	-	-	7.8±2.6	A	86±33
4	81.40	-	16.00	2.50	-	0.10	10.9±2.8	A	73±15
5	-	84.00	16.00	-	-	-	-*	-*	-*
6	-	83.90	16.00	1.25	-	0.10	-*	B	90±10
7	-	81.40	16.00	2.50	-	0.10	-*	C	103±7
8	61.60	-	11.60	1.80	25.00	-	8.1±1.4	A	75±5
9	80.00	-	20.00	-	-	-	7.1±2.2	A	53±35
10	79.90	-	20.00	-	-	0.10	5.6±1.4	A	65±28
11	78.75	-	20.00	1.25	-	-	5.7±0.9	B	111±29
12	77.50	-	20.00	2.50	-	-	8.9±1.5	C	96±46
13	70.00	-	17.50	-	12.50	-	7.5±1.7	A	75±29
14	60.00	-	15.00	-	25.00	-	7.3±1.7	A	34±14
15	50.00	-	12.50	-	37.50	-	4.8±1.2	A	42±2

*: not determinable

Table 2 – Shear viscosity values (η) of selected formulations calculated at the 1.1 s^{-1} shear rate and different temperatures. Tests were carried out on films made of maltodextrins with a dextrose equivalent of 6 (MDX6) or 12 (MDX12) and plasticized by glycerine (GLN) or glycine (GLY)

Form.	Composition (%, w/w)				T	η (Pa*s)
	MDX6	MDX12	GLN	GLY	(°C)	
1	84.00		16.00		100	21000
					110	11600
2	82.75		16.00	1.25	90	7270
					100	7140
					110	6260
3	81.50		16.00	2.50	80	36370
					90	14480
					100	4030
					110	665
5		84.00	16.00		80	39960
					90	19680
					100	3470
					110	2860
9	80.00		20.00		80	14800
					90	3200
					100	2430
					110	540
11	78.75		20.00	1.25	80	5980
					90	4015
					100	1445
					110	513
12	77.50		20.00	2.50	80	8350
					90	5450
					100	1850
					110	800

Table 3 – Tensile properties of formulation 4 (16% w/w glycerine) and 9 (20% w/w glycerine) printed at different filling angles (mean ± St.Dev., n = 5).

Form.	Filling angle	TS (MPa)	Y (MPa)	E% (%)	TBE (MPa)
4	90°	0.07±0.01	1.29±0.26	441±166	0.17±0.09
	120°	0.06±0.01	0.82±0.30	992±83	0.35±0.05
	135°	0.06±0.01	0.84±0.20	705±118	0.25±0.03
	150°	0.07±0.01	1.17±0.14	602±145	0.29±0.04
	180°	0.11±0.01	1.90±0.09	591±65	0.47±0.06
9	90°	0.37±0.15	8.07±4.69	127±56	0.38±0.14
	120°	0.19±0.05	2.76±1.69	431±155	0.66±0.12
	135°	0.48±0.19	7.62±2.59	139±74	0.41±0.07
	150°	0.45±0.10	10.19±2.91	180±53	0.51±0.09
	180°	0.38±0.20	7.53±2.73	184±88	0.44±0.15

Table 4 – Tensile properties of printed ODF (mean ± St.Dev., n = 5).

Form.	TS (MPa)	Y (MPa)	E% (%)	TBE (MPa)
1	-*	-*	-*	-*
2	-*	-*	-*	-*
3	0.09±0.05	2.44±0.1.87	> 1000	0.38±0.17
4	0.06±0.01	0.82±0.30	992±83	0.35±0.05
5	-*	-*	-*	-*
6	-*	-*	-*	-*
7	-*	-*	-*	-*
8	0.75±0.12	23.13±1.72	71±15	0.30±0.07
9	0.19±0.05	2.76±1.69	431±155	0.66±0.12
10	0.05±0.03	0.81±0.47	312±146	0.05±0.01
11	0.09±0.01	1.37±0.68	423±60	0.32±0.29
12	0.01±0.01	0.13±0.01	414±76	0.02±0.01
13	0.53±0.15	10.91±6.36	142±34	0.56±0.12
14	0.43±0.04	8.83±2.06	160±55	0.51±0.16
15	0.43±0.10	8.68±4.07	86±24	0.28±0.06

*: not determinable

Table 5 – Weight and paracetamol (PAR) content of ODF prepared by 3D printing (mean ± St.Dev., n = 3).

Formulation	ODF weight (mg)	Drug content	
		(mg)	(%, w/w)
8	233±45	73.56±3.90	23.49±0.23
13	175±57	22.06±6.87	11.83±0.36
14	215±4	48.94±8.96	25.10±1.31
15	159±15	48.91±5.76	35.76±0.29

Figure1

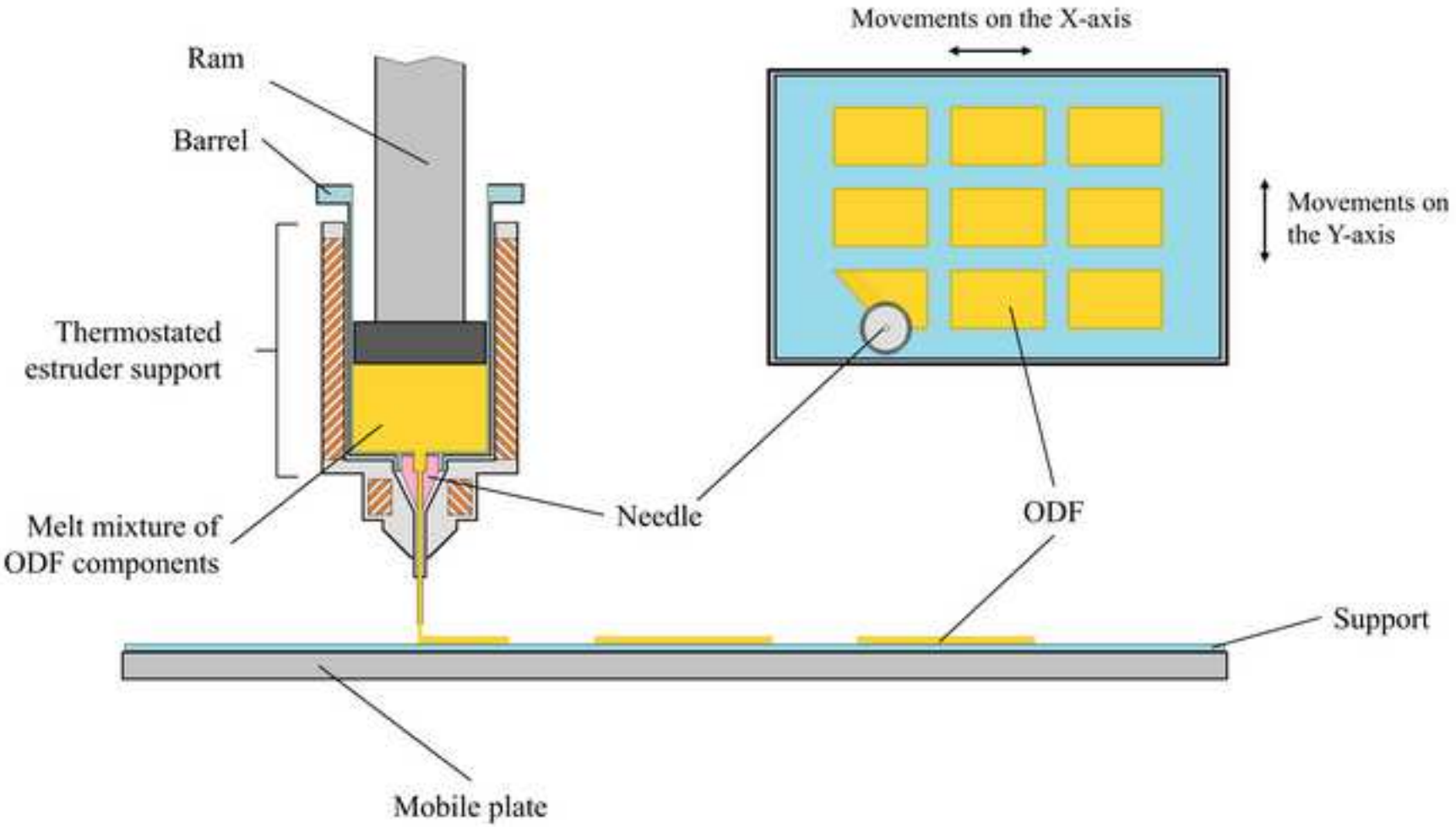
Movements on the X-axis
Ram
Barrel
Movements on
the Y-axis
Thermostated
estruder support
Melt mixture of
ODF components
Needle
ODF
Support
Mobile plate

Figure 2

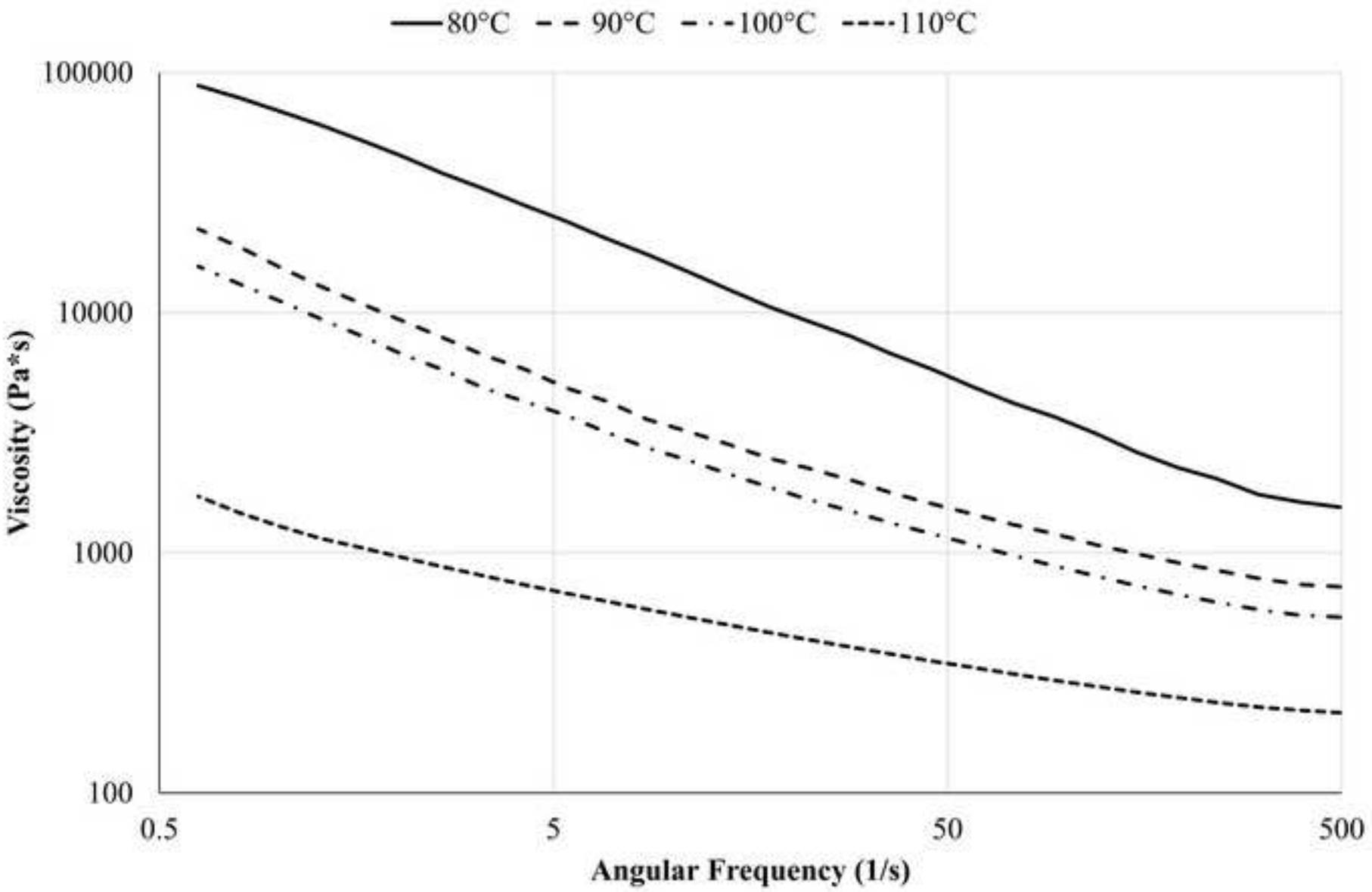
80°C
90°C
100°C
110°C
100000
10000
1000
100
Viscosity (Pa*s)
0.5
5
50
500
Angular Frequency (1/s)

Figure 3

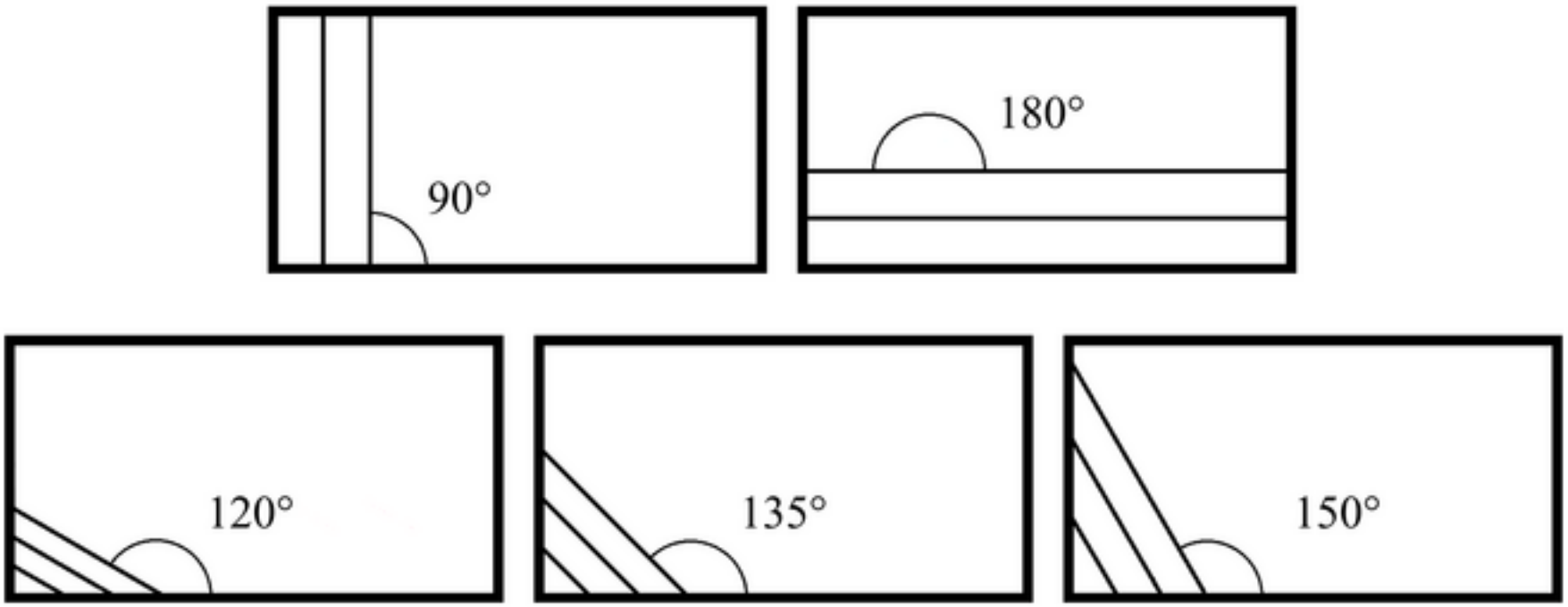

Figure 4

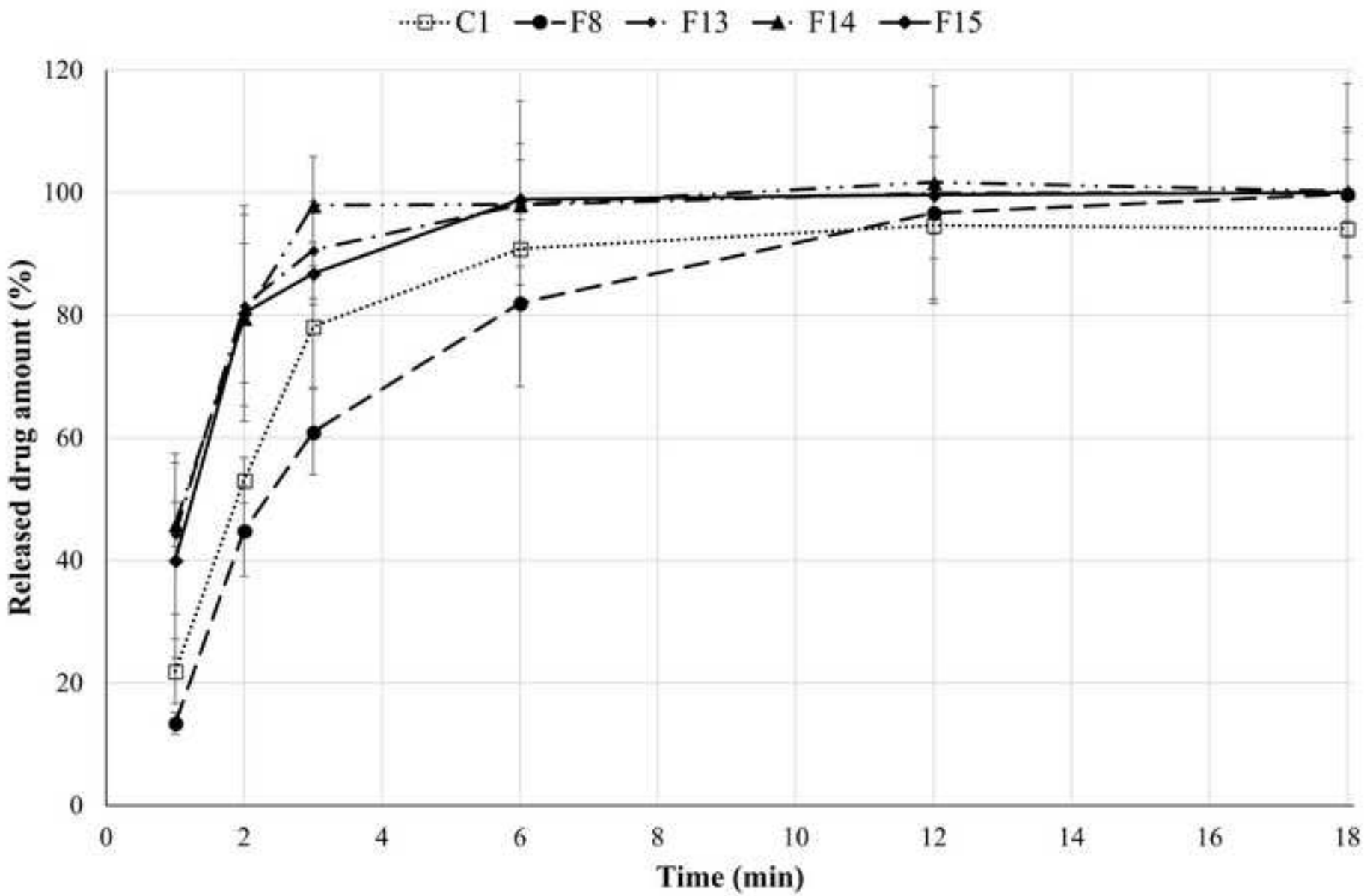
C1
F8
F13
F14
F15
Released drug amount (%)
120
100
80
60
40
20
0
0
2
4
6
8
10
12
14
16
18
Time (min)